Petroleum and Coal

Article **Open Access**

MICRO-SCALE HYDROCARBON DISTRIBUTION IN ORGANIC-RICH SHALES: A CASE STUDY IN THE UNION SPRINGS FORMATION, MARCELLUS SUBGROUP (USA)

EvelynLove Fosu-Duah, Eswaran Padmanabhan, José Antonio Gámez Vintaned*

Department of Geosciences, Department of Geosciences, Universiti Teknologi PETRONAS, Perak, Malaysia

Received June 22, 2017; Accepted October 4, 2017

Abstract

The high economic pressures have shifted the interest in shale resource plays from gas to gas condensates and oil. Geochemically, this is a shift in research perspective from mere knowledge of the organic carbon content of the host rock to the kind, maturity, and extent of heterogeneities in the distribution of the organic components of the shale. This is critical due to the direct relationship between organic carbon and gas storage, transport and deliverability. To investigate the extent of heterogeneities in the hydrocarbon distribution, a combination of Fourier transform infrared spectroscopy, total organic carbon analysis, and ultra-violet infrared spectroscopy were utilized. Shale for the study was sampled from the Union Springs Formation of the Marcellus Subgroup in Pennsylvania. Data analyses from a 10 x 10 cm grid locations show a range of total organic carbon values from 7.51% to 8.96% and an average of 8.13%. Every sample was dominated by aromatic hydrocarbons with E4: E6 values ranging from 2.96 and 3.66. In terms of functional groups, sporadic changes in hydrocarbon bonds were reported. These ranged from the presence of methyl or methylene a/symmetric aliphatic hydrocarbons to aromatic combination C-H, C=C stretching bonds at relatively short intervals. Heterogeneities in the kinds of hydrocarbon reported and their distributions were attributed to the variations in the paleoenvironmental redox conditions, source material, complex depositional history, temporal variations and varying sedimentation rates.

Keywords: *Appalachians; Aromatics; Aliphatics; Organic Carbon.*

1. Introduction

Elucidating the amount, type, maturity, and heterogeneities in the distribution of organic carbon in shales are of great significance due to the potentially recoverable hydrocarbon content of shale gas reservoirs [1-5]. Shale unconventional systems are source rocks that also function as reservoirs, and are a class of continuous hydrocarbon accumulations [6] that are mostly vast, locked in fine-grained low permeability matrices and depend on fracture permeability for production [7]. Gas recovery factors are commonly low [6]. Since their emergence and the first production in the nineteenth century in Fredonia, New York, the demand for the economically viable, shale gas hydrocarbon resources has heightened due to the ever-increasing percentage demand to natural gas and the lack of new conventional resources [8].

Despite exploration and exploitation successes such as, the over 39,500 shale gas wells in the United States of America (USA), production of 600 bcf/year [9], 60% of assessed shale gas resources in the Asian- Pacific regions, the recoverable reserves of 862 trillion cubic feet (tcf) in North America [10], and the 7795 (tcf) throughout the world [11] due to the recent technological advancements in fracking [12-14], recovery rates have remained extremely low (estimated to be about 10% to 30% of gas in place (GIP) [15]. The U.S. government's Energy Information Administration (EIA) predicts that about 46% of the United States' natural gas supply may come from gas shale by 2035, but many other studies confidently point to higher

decline rates of most producing shale gas wells [16-18]. These are indicative of an ultimately possible much lower gas production than it is being projected by the EIA [19-21].

The decline in gas production rates though very unfortunate, it is not surprising due to the fact that, gas shales are extremely complex rocks, characterized by heterogeneities in composition and structure at all scales [18, 22]. This makes the production of gas from shale to be controlled by phenomena acting at many different scales, as have been reviewed by several authors [22-26]. The potentially significant properties impacting production from these reservoirs are the organic carbon content and the hydrocarbon type. These are also known to be related to many petrophysical properties of shale reservoirs. Many studies [1, 27-29] in the United States have identified various interdependence between total organic carbon (TOC), maturity, mineralogical composition, porosity, permeability, grain size and thickness, all of which are also key parameters in shale gas resource assessments and evaluation. For instance, micropore volume has been shown to increase with maturity due to the generation of pores hosted in organic matter [25, 30-31]. There also exists a positive correlation between TOC and porosity [32-33], and then an inverse relationship between TOC and grain size [34-36].

As a typical shale reservoir combines an organic-rich deposition with extremely low matrix permeability [23, 25, 37-38], quantifying and qualifying each of these parameters is key to understanding the potential, the rates, and mechanisms by which gas is delivered from shale to the production wells [39]. Not only are there relatively few detailed studies of hydrocarbon distribution in shales [40-43] but also, the resulting complex organic and inorganic interactions which result in wide variations in surface chemistry [44-46] and sorption issues, each of these is critical to an accurate assessment and design of effective production strategies. Since recent studies place the Marcellus Subgroup as one of the six key gas shale units that account for about 95% of and all domestic oil and natural gas production growth respectively in the USA [47], this paper seeks to contribute to knowledge by making an inventory of the extent of the micro-variations in organic carbon content, aromaticity, hydrocarbon types and their distribution in the Union Springs Formation.

2. Geological setting

2.1. Tectonics

The Palaeozoic history of the Appalachian basin consists of three orogenic events induced by collisions between the North American plates (Laurentia) and the Eastern Oceanic Crust, converting the region from a passive margin during the Ordovician to a foreland basin and a narrow seaway [48]. At various periods, the basin was the site of restricted circulation and accumulation of organic-rich units (e.g., Utica-Point Pleasant and Marcellus Subgroup). The Acadian Orogeny, beginning in the Middle Devonian, resulted in subsidence near the Acadian mountains and uplift on the opposite side caused by flexural deformation [49].

During the Middle and Late Devonian, the Appalachian foreland basin was bounded by the developing Acadian mountains on the east and south, the Cincinnati arch on the west, and the Old Red Sandstone continent to the north, and it was connected to the Rheic Ocean by a long and narrow seaway in the southwest, forming a nearly enclosed epicontinental sea [50-51]. Tectonic loading stemming from this event coupled with eustatic sea level rise terminated shallow-shelf carbonate deposition during the Early Devonian and led to the accumulation of several organic-rich shale units, including the Marcellus Subgroup.

2.2. Stratigraphy

The stratigraphy of the Appalachian basin based on outcrop studies integrated with cores, well logs, and limited geochemical data to construct a sequence-stratigraphic and depositional model is detailed in [52], so that only a brief description is presented here. The Marcellus Subgroup overlies the Eifelian Stage Onondaga Limestone [53]. It comprises of organic- and pyrite-rich black to dark gray shale intervals that are separated by a succession of limestone and sandstone of variable thicknesses [54]. The Marcellus Subgroup in Pennsylvania is divided into three units [55], the first black shale interval is the highly organic carbon-rich Union Springs

Formation [56] and is generally characterized in well logs by a pronounced increase in gamma-ray signatures. The contact between the Onondaga Limestone and the Union Springs Formation is defined as a regional unconformity in the eastern parts of the basin and amalgamated with the Walbridge unconformity in the northeastern portion of the basin, but it is conformable in central Pennsylvania and New York [57].

The Union Springs Formation is overlain by the Cherry Valley Member in Western New York [58], the Purcell Limestone in West Virginia and Pennsylvania [59], and by the Turkey Ridge Member with which it also interfingers in Eastern Pennsylvania [53].

The Cherry Valley Member is composed of nodular and bedded limestone, shale, and siltstone in central and Western Pennsylvania, and the Turkey Ridge Member is composed primarily of sandstone [53]. The Cherry Valley Member and the entire Union Springs Formation are missing along the Northeast-Southwest trending region of western New York and North-Western Pennsylvania, most likely as a result of erosion or non-deposition [57]. The Cherry Valley Member is overlain by the Chittenango Member [56], which is comprised of shale and irregularly interbedded limestone layers [52]. The basal interval of the Chittenango is characterized as having a radioactive (gamma ray) spike, the amplitude of which decreases when moving up in the section. Density also increases up in the section, suggesting an overall decrease in organic carbon concentration within the Chittenango Member [52].

3. Materials and methods

3.1. Materials

The single shale sample for this study is from the Union Springs Formation of the Marcellus Subgroup (Pennsylvania, USA). Six sample locations (labeled P^1 to P^6) were drilled at different points of the shale specimen-in a 10 x 10 cm grid- and evaluated. Sample locations are as presented in Figure 1.

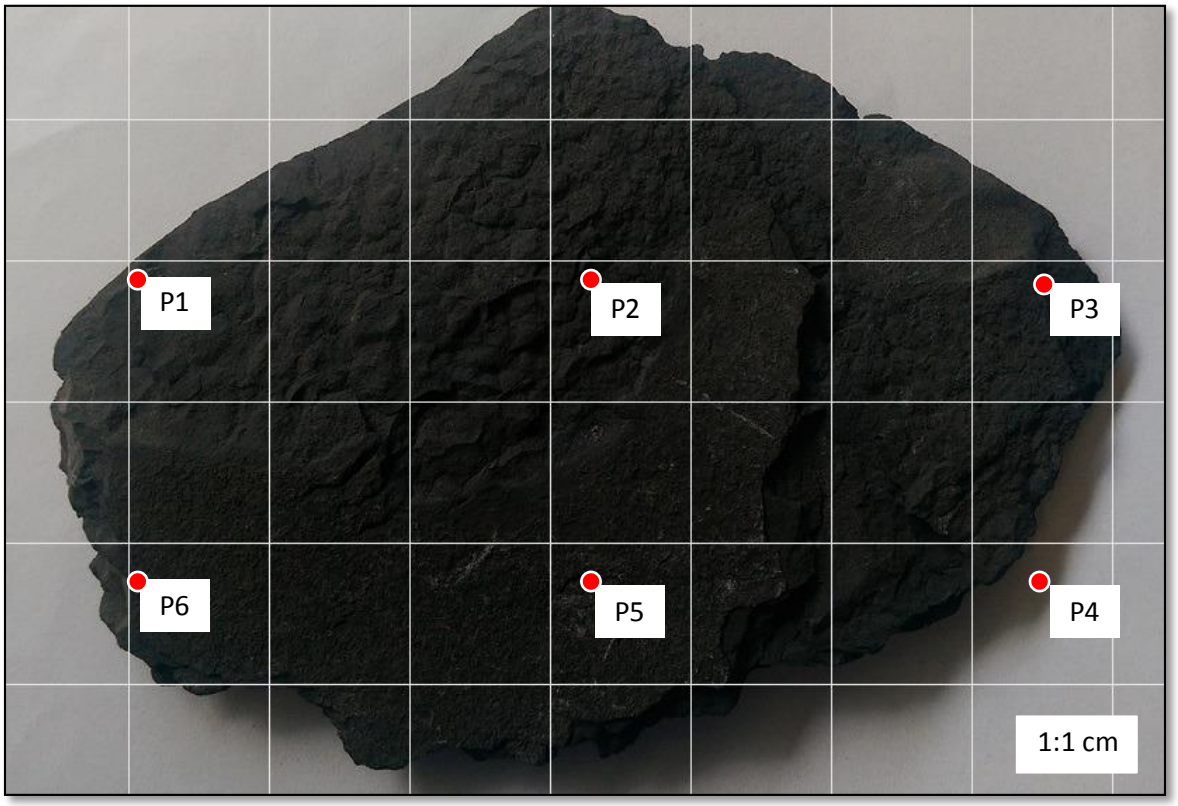

Figure 1. Shale grid showing sample locations

3.2. Total organic carbon (TOC)

TOC analysis to determine the percent weight of organic carbon was measured on powdered shale with a Multiwin analyticjena (Multi N/C 3100) TOC/TNb analyzer adopting the direct method proposed by Dow and Pearson [60]. About 60 mg of pulverized rock pretreated with 10% hydrochloric acid to remove inorganic carbon (carbonates) was used for the analysis. The residual materials were used for the determination of the TOC by combustion analysis of temperatures in excess of 850 °C. The evolved gas (CO) was measured quantitatively and simultaneously by infrared detectors and recorded as the percentage of carbon. The TOC is reported on a dry weight basis [60].

3.3. Ultraviolet-Visible (UV-vis) spectroscopy

UV-vis spectroscopy was performed on dichloromethane extracted hydrocarbon using a Shimadzu UV-3150 spectrophotometer adopting procedures described in Schnitzer and Neyroud [61], Stevenson [62], and then Ramli and Padmanabhan [63]. The primary interest for this analysis was to know the aromaticity; that is, the ratios of aromatic (E4) to aliphatic (E6) hydrocarbon components at the wavelengths of 465 nm and 665 nm respectively at each sample location (Figure 1).

3.4. Fourier-Transform Infrared (FTIR) spectroscopy

Fourier transform infrared (FTIR) spectroscopy to analyze the organic functional groups was performed on an Agilent Technologies Cary 660 Series FTIR Spectrometer. About 2 mg and 0.5 mg of sample were dispersed in PIKE MIRACLE diamond attenuated total reflectance spectroscopy (ATR) to record optimal spectra in the regions of 4000 cm^{-1} to 500 cm^{-1} with a resolution of 4 cm^{-1} and 64 scans.

A quartz beam splitter contained in the spectrometer allowed measurements within the range of 4000 cm^{-1} to 500 cm^{-1}. Spectral manipulation such as baseline adjustment and smoothing was performed using a Spectrocalc software package (Galactic Industries Corporation, NH, USA). Interested functional groups identified in results were identified based on standards in Stuart [64] and Coates [65].

4. Results and discussion

4.1. Hand specimen description

Grain size: Texturally speaking, the studied sample is a lutite i.e. fine grained sedimentary rock composed of clay-sized particles (Figure 2).

Figure 2. Photograph of the Union Springs formation under study

The fine size of its constituent grains may suggest that sediments underwent long periods of suspension in relatively quiet, low energy conditions. Such grains had little chances of becoming rounded due to their small nature and little probability of impact against other grains which would normally cause abrasion and rounding. There are a number and variety of depositional settings where this kind of sediment – often transported as windblown dust – can accumulate, such as in quiet lakes and swamps, at the distal end of a delta (i.e., the prodelta), or at oceanic abyssal plains. The fine-grained nature of the original sediment may also suggest a relatively high organic carbon content due to their hydrodynamic equivalence [66-67].

Fissility: This rock property is as the result of the tendency of clay minerals to be deposited with their sheet structures [(001) crystallographic planes] parallel to the depositional surface, oriented perpendicular to the maximum principal stress direction due to lithostatic pressure. Fissility in the shale is indicative of abundance of clay minerals and organic matter, and the extent of that directly relates to the quantity of the two latter. That is, the more clay minerals in a sediment, the more likely is the resulting shale to become fissile. The degree of preferred orientation of the clay minerals in the shale (fissility) is also known to be related to the electronegativity of the particulate matter in suspension. This is because clay particles tend to adhere to one another if they collide during transport. Adhesion of small mineral grains is referred to as flocculation. If the clay minerals flocculate, then they are less likely to have a preferred orientation, and it is thus less likely to form rocks with fissility like the one in the shale studied herein. One way clay minerals do not adhere to one another but repel in a colloid is when surface potential is relatively high and negative.

Carbonate minerals: The sample fizzed with 10% (HCl). This is an indication of the presence of carbonate minerals. The commonest in the Union Spring Formation is calcite and is known to originate either from digenesis or as bioclastic grains produced by foraminifera and other microorganisms.

Colour: The colour shows varying degrees of hues of black with strands of grey. Although the colour of the shale is not a good classification tool, the opacity of the color black in shale is known to be directly related to the total organic carbon. More often than not, black shale often reports organic carbon of about 2%, which would not be expected to accumulate in shallow, oxygenated water. The color also suggests a rapid sediment burial which can lead to reducing conditions and preservation of carbon compounds in the rock. The varying degrees in the hues of the colour black suggest varying degrees of organic carbon content in the shale. A dominant black colour may suggest either anoxic paleoenvironmental conditions during deposition or anoxia reached shortly after the burial. The varying degrees of opacity in the hues may indicate slight variations in those conditions

4.2. Total organic carbon

Results from the TOC analysis are presented in Figure 3. TOC values range from 7.51% to 8.96%.

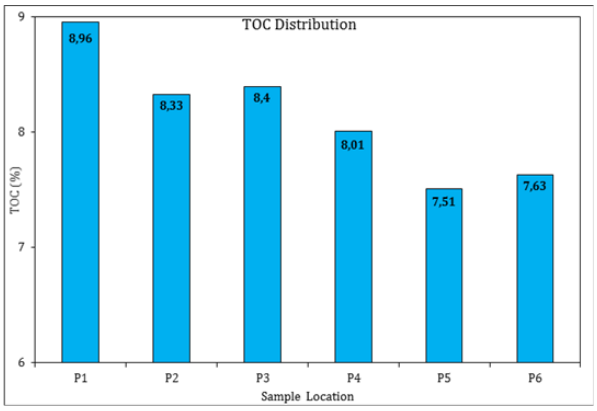

Figure 3. TOC Distribution at Sample Locations

The average TOC value in the sample is 8.13%, which compares well with published data [66-69]. All the sample locations are organic-rich, with an average TOC value which qualifies the specimen as an excellent source rock, that is having TOC values greater than 4% [70]. Variations in the TOC values are slight within the shale sample. It is worth mentioning that significant variations were observed across sample lamella but fairly homogenous among sample locations found along a similar lamella. These observations depict alternating levels of micro-temporal redox conditions and diffe-

rent sedimentation and burial rates. This may explain the decrease in the TOC values in P5 and P6 that are located on a different lamella. They also suggest slight variations in the quality of organic debris or composition that were deposited, as such an expected variations in the susceptibility to degradation and/or remineralization [71].

4.3. Ultra-violet visible (UV-vis) spectroscopy

To characterize the hydrocarbons and determine how variable by type they are distributed along and across the shale lamellae, data from UV-vis was analyzed. The primary avidity was mainly the ratio of optical densities of dilute humic and fulvic acids at wavelengths of 465 nm (E4) and 665 nm (E6) respectively [72-73].

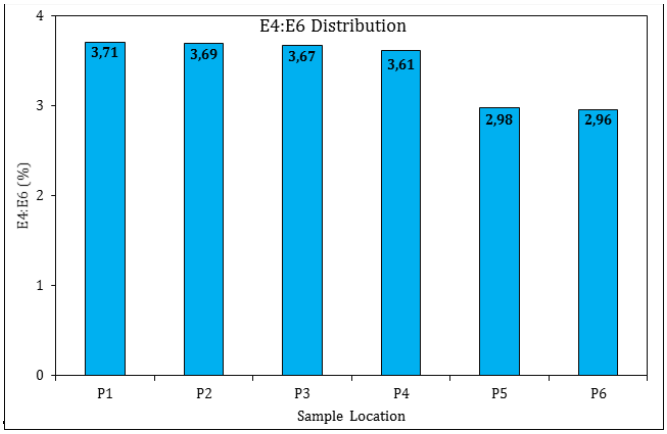

Figure 4. Showing data from E4:E6 values spectroscopy

Results from the analyses presented in Figure 4 show the dominance of aromatic hydrocarbons (E4: E6>1) in all the studied locations (P1-P6). E4: E6>1 range from 2.96 to 3.66 with an average of 3.44. Slight varia-tions in the absolute E4: E6 values are indi-cations of micro-scale heterogeneities in the quality of hydrocarbons within the shale sam-ple. These are reflections of the diverse sedi-mentological conditions during deposition. These slight hetero-geneities suggest differential retention capacities of aromatic compounds within and across rock layers and the shale at large. Variations in the aromaticity suggest preferential migration of the lighter aliphatic components from the shale. These variations in the content of aromatic compounds (E4: E6>1) depicts slight temporal and spatial heterogeneities in thermal maturity and subsequently micro scale pore volume.

4.4. Fourier transform infrared spectroscopy

Data from FTIR analysis are summarized in Table 1. There are somewhat homogenous attri-butes in the type, kind, and intensities in only two locations P1 and P2 (Figure 5). The profiles of P1 and P2 superimpose perfectly; a signature that is as expected due to the relatively small distance between the sample locations. Common functional groups identified at these two locations are low free O-H stretching bonds at 3600 cm^{-1} (Table 1). Such peaks are known to be associated with either water and/or clay minerals. If the latter is true, they may be arising from frequencies associated with the internal surfaces of hydroxyl groups of the clays [74-76].

The distinguishable absorption doublets of aromatic combination C-H stretching bands were identified at the wavelengths of 2340 cm^{-1} and 2360 cm^{-1}. Signatures of aromatic and aliphatic olefin peaks were absorbed in 1500 cm^{-1} and 1600 cm^{-1} respectively. Aromatic (C-H) out of plane bending peaks at wavelengths from 1085-694.33 cm^{-1} were consistent at the two locations. Readings from P3 mimicked the FTIR profile patterns of analyses at points P1 and P2. Slight heterogeneities are the relatively high peak intensities in P3 and the absence of the aromatic –C-H absorbance at 2340 cm^{-1} and 2360 cm^{-1} (Figure 5) which may explain the relatively low E4/E6 value reported at that location.

At P4 to P6 (Figure 6), the characteristic absorption peaks of free O-H stretching, aromatic C=C, aliphatic =C-H and out of plane C-H bending at wavelengths of 3600 cm^{-1}, 1500 cm^{-1}, 1600cm^{-1} and 1085-694 cm^{-1} respectively (Figure 3) were all observed like in the other three locations (P1 to P3) (Figure 5). Slight changes in peak positions may indicate variable ring-substitution patterns [64, 77]. Variations in the peak positions and intensities in the bands of the out of plane bending vibrations of aromatic compounds at wavelengths between 900 cm^{-1} to 700 cm^{-1} (Table 1) indicate heterogeneities in the number of hydrogens in the aromatic ring [78-80].

Perhaps the astonishing traits of the profiles presented here are the sporadic variations in peak intensities and organic functional groups reported in P4 to P6 (Figure 6) despite their proximity laterally and horizontally to P1 to P3 (Even the distinction between the free O-H stretching regions is clearer at wavelengths of 3695 cm^{-1} and 3620 cm^{-1} characteristics of the kaolin group at these two locations [77]. There is also a broad absorption peak near 3400 cm^{-1} indicative of the clay mineral illite which is absent at P1 to P3). Although the aromatic –C-H absorption doublets at 2340 cm^{-1} and 2360 cm^{-1} are absent at P4 to P6 the aromatic C=C absorption at 1500 cm^{-} seem to be more pronounced than those reported at P1 to P3. Another observation is the absence of the aliphatic olefin peak (=C-H) at 1600 cm^{-1} in only P4 (Table 1; Figure 6). The absorption peaks at the wavelength bands 2960 cm^{-1} to 2930 cm^{-1} and 2870 cm^{-1} to 2850 cm^{-1} indicate the presence of aliphatic methyl and methylene a/symmetric C–H stretching hydrocarbons respectively in P5 and P6 (Table 1, Figure 6). The relatively high concentrations of aliphatic hydrocarbon bonds in P5 and P6 justify their lower reported aromaticity (Figure 4). The profiles of P5 and P6 only differ by transmittance peak intensities. The later seems to report relatively higher transmittances than P5 which according to Coates [65] and Silverstein, *et al.* [81] is an indication of variations in the quantity of that particular functional group. This observation may actually explain the relatively higher aromaticity in P5 despite its lower TOC (Figure 3).

Table 1. Summary of results from FTIR spectroscopy

Functional Group		Sample ID					
		P1	**P2**	**P3**	**P4**	**P5**	**P6**
Bonds	*Type*	*Wavelengths (cm^{-1})*					
Al≡O-H Stretching	Inorganic				3694.12	3695.41	3696.10
Al≡O-H (Inner Octahedral)	Inorganic	3620.60	3620.60	3620.62	3619.63	3650.29	3621.48
H-O-H Stretching	Inorganic	3384.95	3384.95	3398.58		3414.93	3408.35
Methyl symmetric C–H	Aliphatic					2959.61	2960.17
Methylene asymmetric C–H	Aliphatic					2930.34	2928.10
Methyl asymmetric C–H	Aliphatic					2865.19	2865.19
Methylene symmetric C–H	Aliphatic					2843.47	2844.10
C=C stretching	Aliphatic	2161.72	2161.72				
Combination C-H stretching	Aromatic	2360.29	2360.29				
	Aromatic	2340.87	2340.87				
Overtone and combination bands	Aromatic	1983.52	1983.52	1979.78			
C=C stretching	Aromatic	1598.00	1598.00	1634.01	1637.66	1636.91	
	Aromatic	1438.74	1438.74		1431.00	1514.33	
In-plane C-H bending	Aromatic	1004.73	1004.73			1052.63	
	Aromatic					1032.19	
	Aromatic					1007.12	
Out-of-plane C–H bending	Aromatic	913.22	913.22	984.96	996.39		993.98
	Aromatic	777.31	777.31	829.13	795.47	795.79	911.96
	Aromatic	692.99	692.99	692.83	776.84	756.25	828.16
	Aromatic				692.46	692.89	795.31
	Aromatic						777.02
	Aromatic						692.40

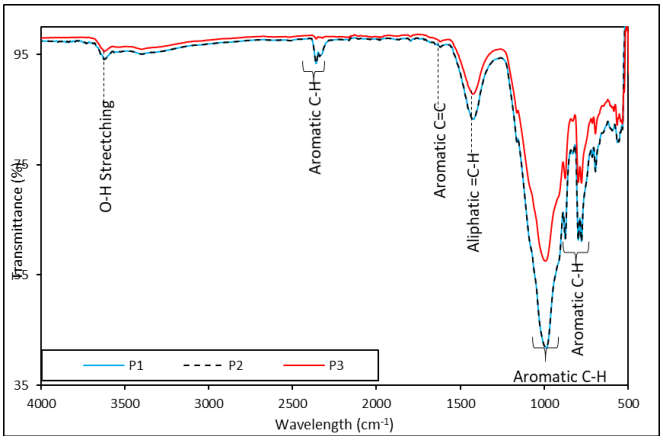

Figure 5. FTIR Spectra of Sample Points P1 to P3

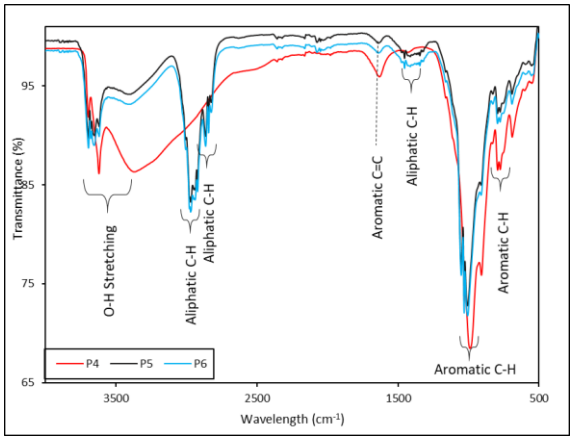

Figure 6. FTIR Spectra of Sample Points P4 and P5

5. Conclusion

This study indicates sporadic changes in organic carbon content, hydrocarbon type, bonds and their distribution in the Union Springs Formation. These variations within a relatively small scale have the potential to change the concept and knowledge of gas storage and transport mechanisms in the studied formation.

Heterogeneities in the amount and type of organic carbon, as well as in the contents of aliphatic and aromatic functional groups at the various locations on the sample, are indicative of slight variations in the source materials and redox conditions which may suggest complicated temporal and spatial depositional patterns.

The fissility of the sample implies a relatively high clay mineralogical content and a high electronegative surface, which in turn suggests the influence of surface potential and organo-complex issues on physicochemical parameters which are in play as the mechanisms of flocculation, sedimentation, and transport take place.

The relatively high organic carbon content and high aromaticity suggest an -in general- anoxic depositional environment. They also suggest the potential of relatively high specific surfaces and a subsequent relatively high adsorption capacities for gas. However, slight heterogeneities in hydrocarbon distribution suggest variations in transport mechanisms at very small scales within the Union Springs Formation, which may mean diverse adsorptions capacities at relatively small distances.

Acknowledgements

The donors of the Petroleum Research Fund offered to A.P. Dr. Eswaran Padmanabhan, administered by the Research and Information Office (RIO) are highly acknowledged for financially supporting this research.

References

[1] Montgomery SL, Jarvie DM, Bowker KA and Pollastro RM. Mississippian Barnett Shale, Fort Worth basin, north-central Texas: Gas-shale play with multi–trillion cubic foot potential. American Association of Petroleum Geologists bulletin, 2005; 89: 155-175.

[2] Loucks RG and Ruppel SC., Mississippian Barnett Shale: Lithofacies and depositional setting of a deep-water shale-gas succession in the Fort Worth Basin, Texas. American Association of Petroleum Geologists bulletin, 2007; 91: 579-601.

[3] Rowe HD, Loucks RG, Ruppel SC and Rimmer SM. Mississippian Barnett Formation, Fort Worth Basin, Texas: Bulk geochemical inferences and Mo–TOC constraints on the severity of hydrographic restriction. Chemical Geology, 2008; 257: 16-25.

[4] Ross DJK and Bustin RM. Impact of mass balance calculations on adsorption capacities in microporous shale gas reservoirs. Fuel, 2007; 86: 2696-2706.

[5] Jarvie DM, Hill RJ, Ruble TE, Pollastro M. Unconventional shale-gas systems: The Mississippian Barnett Shale of north-central Texas as one model for thermogenic shale-gas assessment. *A*merican Association of Petroleum Geologists bulletin, *2007;* 91(4): 475-499.
[6] Schmoker JW. Resource-assessment perspectives for unconventional gas systems. American Association of Petroleum Geologists bulletin, 2002; 86: 1993-1999.
[7] Nielson DH. Method and apparatus for shale gas recovery. ed: Google Patents, 1990.
[8] Zhao T, Li X, Zhao H and Dou X. Micro-storage State and Adsorption behavior of Shale Gas. Society of Petroleum Engineers. doi:10.2118/178386-MS.
[9] EIA. Technically recoverable shale oil and shale gas resources: An assessment of 137 shale formations in 41 countries outside the United States. in Energy Information Administration, US D of Energy, Ed., ed. Washington. DC, 2014.
[10] Boyer C, Clark B, Jochen V, Lewis R and Miller CK. Shale gas: a global resource. Oilfield review, 2011; 23: 28-39.
[11] Guo J and Zhao Z. China vigorously promoting shale gas exploration, development. Oil and Gas Journal, 2012; 110: 1-10.
[12] Soltanzadeh M, Davis G, Fox A, Hume D and Rahim N. Application of mechanical and mineralogical rock properties to identify fracture fabrics in the Devonian Duvernay formation in Alberta. Unconventional Resources Technology Conference, San Antonio, Texas, 20-22 July 2015.
[13] Sun J and Schechter D. Investigating the Effect of Improved Fracture Conductivity on Production Performance of Hydraulically Fractured Wells: Field-Case Studies and Numerical Si-mulations. Journal of Canadian Petroleum Technology, 2015; 54(06) doi:10.2118/169866-PA.
[14] Sun H, Chawathe A, Hoteit H, Shi X and Li L. Understanding shale gas flow behavior using numerical simulation. Society of Petroleum Engineers Journal2015; 20: 142-154.
[15] Wu K, Li X, Wang C, Yu W, Guo C, Ji D, et al., Apparent Permeability for Gas Flow in Shale Reservoirs Coupling Effects of Gas Diffusion and Desorption. Unconventional Resources Technology Conference, 25-27 August, Denver, Colorado, USA., doi.org/10.15530/URTEC-2014-1921039
[16] JD Baihly, R Malpani, C Edwards, SY Han, JCL Kok, EM Tollefsen, Wheeler CW. Unlocking the shale mystery: How lateral measurements and well placement impact completions and resultant production. presented at the Tight Gas Completions Conference, 2010, ISBN: 9781617820403.
[17] Baihly JD, Altman RM, Malpani R and Luo F. Shale gas production decline trend comparison over time and basins," presented at the Annual Technical Conference and Exhibition, 2010.
[18] Jarvie DM, Hill RJ, Ruble TE and Pollastro RM. Unconventional shale-gas systems: The Mississippian Barnett Shale of north-central Texas as one model for thermogenic shale-gas assessment. AAPG bulletin, 2007; 91: 475-499.
[19] Conti J, Holtberg P, Beamon J, Napolitano S and Schaal A. Annual energy outlook 2013 with projections to 2040 US. Energy Information Administration, vol. EIA-0383, 2013.
[20] Dong Z, Holditch SA and McVay DA. Resource Evaluation for Shale Gas Reservoirs. SPE Economics & Management, 2012 ; 5(01).
[21] Boulis A, Jayakumar R, Lalehrokh F and Lawal H. Improved Methodologies for More Accurate Shale Gas Assessments. 2012.
[22] Sondergeld CH, Newsham KE, Comisky JT, Rice MC and Rai CS. Petrophysical considerations in evaluating and producing shale gas resources. 2010.
[23] Loucks RG, Reed RM, Ruppel SC and Jarvie DM. Morphology, genesis, and distribution of nanometer-scale pores in siliceous mudstones of the Mississippian Barnett Shale. Journal of sedimentary research, 2009; 79: 848-861, 2009.
[24] Wang FP and Reed RM. Pore networks and fluid flow in gas shales. 2009.
[25] Ross DJ and Bustin RM. Characterizing the shale gas resource potential of Devonian–Mississippian strata in the Western Canada sedimentary basin: Application of an integrated formation evaluation. American Association of Petroleum Geologists bulletin, 2008; 92: 87-125.
[26] Bustin RM, Bustin AMM, Cui A, Ross D and Pathi VM. Impact of shale properties on pore structure and storage characteristics. Presented at the Shale Gas Production Conference, 2008.
[27] Harris LD, de Witt W Jr and Colton GW. What are possible stratigraphic controls for gas fields in eastern black shale. Oil Gas J., 1970; 76.

[28] Cluff RM and Dickerson DR. Natural Gas Potential of the New Albany Shale Group (Devonian-Mississippian) in Southeastern Illinois. Society of Petroleum Engineers Journal, 1982; 22: 291-300.
[29] Pollastro RM, Hill RJ, Jarvie DM and Henry ME. Assessing undiscovered resources of the Barnett-Paleozoic total petroleum system, Bend Arch-Fort Worth basin province, Texas. 2003.
[30] Loucks RG, Reed RM, Ruppel SC and Hammes U. Spectrum of pore types and networks in mudrocks and a descriptive classification for matrix-related mudrock pores. American Association of Petroleum Geologists bulletin, 2012; 96: 1071-1098.
[31] Zhang T, Ellis GE, Ruppel SC, Milliken K, Lewan M and Sun X. Effect of Organic Matter Properties, Clay Mineral Type and Thermal Maturity on Gas Adsorption in Organic-Rich Shale Systems. 2013.
[32] H Tian, L Pan, T Zhang, X Xiao, Z Meng and B. Huang Pore characterization of organic-rich Lower Cambrian shales in Qiannan Depression of Guizhou Province, Southwestern China. Marine and Petroleum Geology, 2015; 62: 28-43.
[33] Milliken KL, Rudnicki M, Awwiller DN and Zhang T. Organic matter–hosted pore system, Marcellus formation (Devonian), Pennsylvania. American Association of Petroleum Geologists Bulletin, 2013; 97: 177-200.
[34] Mayer LM. Surface area control of organic carbon accumulation in continental shelf sediments," Geochimica et Cosmochimica Acta, 1994; 58: 1271-1284.
[35] Christensen BT. Physical fractionation of soil and organic matter in primary particle size and density separates. in Advances in soil science, ed: Springer, 1992: 1-90.
[36] Kennedy MJ, Pevear DR and Hill RJ. Mineral surface control of organic carbon in black shale. Science, 2002; 295: 657-660.
[37] Akkutlu IY and Fathi E. Multiscale gas transport in shales with local kerogen heterogeneities. Society of Petroleum Engineers Journal, 2012; 17: 1-002.
[38] Luffel DL, Hopkins CW and Schettler Jr PD. Matrix permeability measurement of gas productive shales. 1993.
[39] Ambrose RJ, Hartman RC, Diaz-Campos M, Akkutlu IY and Sondergeld CH. Shale gas-in-place calculations part I: new pore-scale considerations. Society of Petroleum Engineers Journal, 2012; 17: 219-229.
[40] Chalmers GRL and Bustin RM. The organic matter distribution and methane capacity of the Lower Cretaceous strata of Northeastern British Columbia, Canada. International Journal of Coal Geology, 2007; 70: 223-239.
[41] Chareonsuppanimit P, Mohammad SA, RobinsonJr RL and Gasem KAM. High-pressure adsorption of gases on shales: Measurements and modeling. International Journal of Coal Geology, 2012; 95: 34-46.
[42] Gasparik M, Bertier P, Gensterblum Y, Ghanizadeh A, Krooss BM and Littke R. Geological controls on the methane storage capacity in organic-rich shales. International Journal of Coal Geology, 2014; 123: 34-51.
[43] AS Pepper and PJ. Corvi Simple kinetic models of petroleum formation. Part I: oil and gas generation from kerogen. Marine and Petroleum Geology, 199; 12: 291-319.
[44] Fosu-Duah EL, Padmanabhan E and Vintaned JAG. Electrophoretic behavior of some shales from the setap formation, Sarawak Basin, Malaysia. International Journal of Applied Engineering Research, 2016; 11. 337-341.
[45] Fosu-Duah EL, Padmanabhan E and Vintaned JAG. Variations in specific surface area of some Oligocene-Miocene shales. Journal of Scientific Research and Development, 2016; 3: 33-43.
[46] Fosu-Duah EL, Padmanabhan E and Vintaned JAG. Characteristic Zeta Potential of Selected Oligocene-Miocene Shales from the Setap Formation, Onshore Sarawak-Malaysia. International Journal of Applied Engineering Research, 2017; 12: 6360-6368.
[47] Yu W, Sepehrnoori K and Patzek TW. Evaluation of Gas Adsorption in Marcellus Shale. 2014.
[48] van Staal CR, Whalen JB, Valverde-Vaquero P, Zagorevski A and Rogers N. Pre-carboniferous, episodic accretion-related, orogenesis along the laurentian margin of the northern appa-lachians. in Anciemt orogens and modern analogus. vol. 327, J. B. Murphy, J. D. Keppie, and A. J. Hynes, Eds., ed London: Geological Society Special Publication, 2009, pp. 271-316.
[49] Warner NR, Jackson RB, Darrah TH, Osborn SG, Down A, Zhao K. Geochemical evidence for possible natural migration of Marcellus Formation brine to shallow aquifers in Pennsylvania. Proceedings of the National Academy of Sciences, 2012; 109. 11961-11966.
[50] Ettensohn FR. The Catskill delta complex and the Acadian orogeny: A model. Geological Society of America Special Papers, 1985; vol. 201: 39-50.

[51] Castle JW. Appalachian basin stratigraphic response to convergent-margin structural evolution. Basin Research, 2001; 13: 397-418.
[52] Lash GG and Engelder T. Thickness trends and sequence stratigraphy of the Middle Devonian Marcellus Formation, Appalachian Basin: Implications for Acadian foreland basin evolution. American Association of Petroleum Geologists Bulletin, 2011; 95: 61-103.
[53] Kohl D, Slingerland R, Arthur M, Brach R, and Engelder T. Sequence stratigraphy and depositional environments of the Shamokin (Union Springs) Member, Marcellus Formation, and associated strata in the middle Appalachian Basin. American Association of Petroleum Geologists Bulletin, 2014; 98: 483-513.
[54] Rickard LV. Correlation of the Devonian rocks in New York State: New York State Mus. and Sc. Service Geol. Survey Map and Chart Ser, 1964; vol. 4.
[55] Ver Straeten CA. Basinwide stratigraphic synthesis and sequence stratigraphy, upper Pragian, Emsian and Eifelian stages (Lower to Middle Devonian), Appalachian Basin. Geological Society, London, Special Publications, 2007; vol. 278: 39-81.
[56] Cooper GA. Stratigraphy of the Hamilton group of New York. American Journal of Science, 1930: 116-134.
[57] Johnson JG, Klapper G and Sandberg CA. Devonian eustatic fluctuations in Euramerica. Geological Society of America Bulletin, 1985; 6: 567-587.
[58] Clarke JM. Classification of New York Series of geologic formations: New York State Museum, 1903.
[59] Cate AS. Lithostratigraphy of some Middle and Upper Devonian rocks in the subsurface of southwestern Pennsylvania. 1963.
[60] Dow WG and Pearson DB. Organic Matter In Gulf Coast Sediments. Presented at the Offshore Technology Conferences, 1975.
[61] Schnitzer M and. Neyroud JA Further investigations on the chemistry of fungal "humic acids". Soil Biology and Biochemistry, 1975; 7: 365-371.
[62] Stevenson FJ. Humus chemistry; genesis, composition, reactions. 1982.
[63] MS Raml, and E. Padmanabhan. Heterogeneity of the hydrocarbon distribution in tertiary sediments of north-east Sarawak. Presented at the International Petroleum Technology Conference, Thailand, 2011.
[64] Stuart B. Infrared spectroscopy: Wiley Online Library, 2005.
[65] Coates J. Interpretation of Infrared Spectra, A Practical Approach. In Encyclopedia of Analytical Chemistry. vol. 12, R. A. Meyers, Ed., ed Chichester UK: John Wiley & Sons, Ltd, 2002, pp. 10815–10837.
[66] Bruner KR and Smosna R. A comparative study of the mississippian barnett shale, fort worth basin, and Devonian marcellus shale, appalachian basin. USA: U.S. Department of energy, 2011.
[67] Zielinski RE and Nance SW. Physical and chemical characterization of Devonian gas shale. Quarterly Status Report vol. MLM-EGSP-TPR-Q-009, p. 166, 1979.
[68] Wendt AK, Arthur MA, Slingerland R, Kohl D, Brach R, and Engelder T. Geochemistry and depositional history of the Union Springs Member, Marcellus Formation in central Pennsylvania. Interpretation, 2015; 3: SV17-SV33.
[69] Sageman BB, Murphy AE, Werne JP, Ver Straeten CA, Hollander DJ and Lyons TW A tale of shales: the relative roles of production, decomposition, and dilution in the accumulation of organic-rich strata, Middle–Upper Devonian, Appalachian basin. Chemical Geology, 2003; 195:229-273.
[70] Peters KE and Cassa MR. Applied Source Rock Geochemistry: Chapter 5: Part II. Essential Elements," 1994.
[71] Hedges JI and Keil RG Sedimentary organic matter preservation: an assessment and speculative synthesis. Marine Chemistry, 1995; 49: 81-115.
[72] Evdokimov IN and Losev AP Potential of UV-visible absorption spectroscopy for characterizing crude petroleum oils. 2007.
[73] Mullins OC. Optical interrogation of aromatic moieties in crude oils and asphaltenes. in Structures and Dynamics of Asphaltenes, ed: Springer, 1998, pp. 21-77.
[74] Madejová J, Pentrák M, Pálková H and Komadel P. Near-infrared spectroscopy: A powerful tool in studies of acid-treated clay minerals. Vibrational Spectroscopy, 2009; 49: 211-218.
[75] Madejova J and Komadel P. Baseline studies of the clay minerals society source clays: infrared methods," Clays and clay minerals, 2001; 49. 410-432.

[76] Davarcioglu B and Ciftci E. The clay minerals observed in the building stones of Aksaray-Guzelyurt area (Central Anatolia-Turkey) and their effects. International Journal of Physical Sciences; 5: 1734-1743.
[77] Farmer VC. Differing effects of particle size and in the infrared and Raman spectra kaolinite shape. Clay Minerals, 1998; 33: 601-604.
[78] Bartick EG. Applications of vibrational spectroscopy in criminal forensic analysis. Handbook of Vibrational Spectroscopy, 2002.
[79] Franke JE. Inverse Least Squares and Classical Least Squares Methods for Quantitative Vibrational Spectroscopy. In Handbook of Vibrational Spectroscopy, ed: John Wiley & Sons, Ltd, 2006.
[80] Miller CE. Near-Infrared Spectroscopy of Synthetic and Industrial Samples. Handbook of Vibrational Spectroscopy, 2002.
[81] Silverstein RM, Webster FX, Kiemle DJ and Bryce DL. Spectrometric identification of organic compounds: John Wiley & Sons, 2014.

To whom correspondence should be addressed: Dr. Eswaran Padmanabhan, Department of Geosciences, Faculty of Geosciences and Petroleum Engineering, Universiti Teknologi PETRONAS, Perak, Malaysia,